



HAL
open science

Geopolymer local network evolution under time and temperature

Julien Archez, Ameni Gharzouni, I. Sobrados, A. Piancastelli, J.F. Caron, N. Texier-Mandoki, Sylvie Rossignol, X. Bourbon

► **To cite this version:**

Julien Archez, Ameni Gharzouni, I. Sobrados, A. Piancastelli, J.F. Caron, et al.. Geopolymer local network evolution under time and temperature. *Journal of Non-Crystalline Solids*, 2021, 566, pp.120870. 10.1016/j.jnoncrysol.2021.120870 . hal-03296195

HAL Id: hal-03296195

<https://unilim.hal.science/hal-03296195>

Submitted on 9 May 2023

HAL is a multi-disciplinary open access archive for the deposit and dissemination of scientific research documents, whether they are published or not. The documents may come from teaching and research institutions in France or abroad, or from public or private research centers.

L'archive ouverte pluridisciplinaire **HAL**, est destinée au dépôt et à la diffusion de documents scientifiques de niveau recherche, publiés ou non, émanant des établissements d'enseignement et de recherche français ou étrangers, des laboratoires publics ou privés.



Distributed under a Creative Commons Attribution - NonCommercial 4.0 International License

GEOPOLYMER LOCAL NETWORK EVOLUTION UNDER TIME AND TEMPERATURE

J. Archez^{1,2,3}, A. Gharzouni¹, I. Sobrados⁴, A. Piancastelli⁵, J.F. Caron³, N. Texier-
Mandoki², X. Bourbon² and S. Rossignol¹

¹ IRCER: Institut de Recherche sur les Céramiques (UMR7315), 12 rue Atlantis, 87068 Limoges, France.

² Agence nationale pour la gestion des déchets radioactifs (Andra), 1/7 rue Jean-Monnet, 92298 Chatenay-Malabry, France.

³ Laboratoire Navier, UMR 8205, Ecole des Ponts Paristech, CNRS, UPE, Champs-sur-Marne,

⁴ Instituto de Ciencia de Materiales de Madrid, Consejo Superior de Inverstigaciones Cientificas (CSIC), C/Sor Juana Inés de la Cruz, 3, 28049 Madrid, Spain.

⁵ CNR - Istituto di Scienza e Tecnologia dei Materiali Ceramici Via Granarolo, 64 I-48018 Faenza (RA), Italy.

■ Corresponding author: sylvie.rossignol@unilim.fr, tel.: 33 5 87 50 25 64

Geopolymer	Aging	Temperature
Structure	Porosity	NMR

Abstract

This study was undertaken in the context of Cigéo project to investigate the use of geopolymer for potential applications in high level waste cell. The aim was to evaluate the structural evolution of potassium metakaolin based geopolymer as a function of time and temperature for geological nuclear waste disposal applications. The evolution of mechanical properties, local structure, and porosity of geopolymer binder and composites stored at 0.5

and 20 months at 20 and 90 °C were studied. It was shown a decrease of density and stability of mechanical strength over time at 20 °C and a slight decrease at 90 °C. Moreover, it was evidenced the stability of the structure over time at 20 °C and the nucleation of a small amount of zeolite type phase at 90 °C. The mesoporosity was favored over time. However, an increase of porosity and pore size was evidenced at 90 °C due to pore coalescence and water removal. A model of aging was proposed in order to elucidate the structural changes over time and temperature. It has been shown that the aging of geopolymer at 20 and 90 °C induces changes of porosity and pore size distribution but seems not to degrade the structure and properties of the final material.

I. INTRODUCTION

Cigéo is the geological disposal facility project for radioactive waste managed by the French National Radioactive Waste Management Agency (Andra) for high-level and long-lived intermediate-level radioactive wastes. If licensed, it will be built 500 m underground in a specific geological layer composed of the Callovo-Oxfordian (COx) argillites, in the East of France. Geopolymers are studied by Andra as potential new materials that can be used in Cigéo for example as grout at the boundary between the geological argillite and the lining of the high-level radioactive waste disposal cell [1], or as composite for the liner to reduce metallic use [2], or as fire-resistant materials [3]. Indeed, geopolymers are inorganic materials consolidated at low temperatures from the activation of an aluminosilicate source and an alkaline solution [4]. These materials are attractive because of their easy synthesis method, high working performance such as high mechanical strength, fire resistance, and wide range of applications [5] and low environmental impact [6]. The use of geopolymer materials requires further comprehension of their evolution over time under different conditions such as temperature and relative humidity. To consider potential applications in high level waste cell,

materials properties have to be determined in conditions representative of the operation (temperature between 20 and 90 °C, humidity, etc.).

The evolution of materials is mainly studied over time, in temperature, relative humidity, and under pressure [7]. For this, several data such as shrinkage, porosity, permeability, and mechanical data are collected over time and temperature [8]. The effect of curing temperature during aging has been investigated by Cioffi et al. [9]. The decrease in strength and density of geopolymer at 60 °C was evidenced. Steins et al. [10] have investigated the porosity with aging. Densification of the solid network and a partial closure of the porosity at the nanometer scale (constriction of some narrow channel) was evidenced. Moreover, the durability can be improved by decreasing porosity and permeability [11]. Greater compressive strength could also be reached with a lesser porosity sample [12]. Other study made by Melar et al. [13] has evidenced that the potassium ions are responsible for the pore structure organization after 2 months and 5 years aging at 20 °C.

Other authors focused on the effect of relative humidity and temperature variation on the local network. For example, Kovalchuk et al. [14] have studied alkali-activated material cured in dry condition (at 150 °C) and in steam condition (at 95 °C with 100 % RH). ²⁹Si NMR data evidenced a higher amount of Al-rich aluminosilicate gel (increase of Q⁴(4Al) species) when the relative humidity increases. It has also been shown that the mechanical resistance has been reduced with dry curing (30 MPa) compared with steam curing (72 MPa) due to the removal of water. The structural evolution of metakaolin-based geopolymers cured at different temperatures (50 and 110 °C) and relative humidity percentages (40 and 100 %) was also studied during 3 weeks and 3 years [15]. It was demonstrated that curing at 110 °C induces a semi-crystalline structure closer to zeolites. Moreover, curing at 40 % of relative humidity leads to a higher amorphous structure than 100 % RH. Moreover, a stable structure is evidenced after 3 years at room temperature.

This work aims to study the evolution of geopolymer composites formulation developed for the lining of the high-level radioactive waste disposal cell at ambient temperature and at 90 °C (which is the temperature that can be reached by the cell in operation). The evolution of mechanical properties, density, and porosity of geopolymer binder and composites stored at 0.5 and 20 months at 20 and 90 °C were studied. The structure of these samples was then analyzed with XRD, FTIR, and NMR measurements.

II. EXPERIMENTAL PART

Raw materials, samples preparation, and storage conditions

A commercial potassium solution provided by Woellner, with silicon to potassium (Si/K) molar *ratio* of 1.70 was modified by dissolving pellets of KOH by magnetic stirring for five minutes to reduce the Si/K molar *ratio* to 0.58. The geopolymer binder was synthesized by dissolving a commercial metakaolin (M1000) provided by Imerys in the silicate alkaline solution to obtain Si/Al molar ratio of 1.62. Based on a previous study [16], acicular particles (L. = 5-170 μm , D. = 3-15 μm) of wollastonite (W) provided by Imerys and/or alkaline resistant glass fibers (G) (L. = 6 mm, D. = 13-15 μm) provided by Owens Corning were also added to form a geopolymer composite. The resulting mixture was mixed until obtaining a homogenous mixture for a total time of ten minutes. Four formulations were studied: a geopolymer binder, named M1, and three geopolymer composites named M1W, M1G, and M1WG elaborated with the addition of a weight percentage (relative to the mass of the binder) of 18 % of wollastonite, 4,5 % of glass fibers, 9 % of wollastonite and 2.25 % of glass fibers. The reactive mixtures were then cast in polystyrene sealed mold. The samples were unmolded after 7 days and stored for 0.5 and 20 months in two storage conditions: (i) at 20 °C in a plastic sealed bag with a relative humidity of 100 % and (ii) at 90 °C in an oven with a relative humidity inferior to 5 %.

Characterization

The pH measurement was made at 20 °C on a consolidated geopolymer (solid) after a 7 days immersion with a pH-meter 3310 WTW as described in previous work [17].

Inductively coupled plasma optical emission spectrometry (ICPOES) was performed using a Perkin Elmer 8300 DV to determine the chemical composition of the solution after immersion of geopolymer. A sampling of 12 ml of solution (diluted 30-fold) was analyzed.

The pores size distribution was analyzed with a collaboration with ISTECH (Italy) on monolith sample by mercury porosimetry (Thermo Finnigan Pascal 140 and Thermo Finnigan Pascal 240) in the range 0.0078 - 100 μm with a surface tension of 0.48 N/m, a contact angle equal to 140° and an experimental error of 4 % due to the accuracy of the instrument.

The microstructure was analyzed with a JEOL IT 300 LV scanning electron microscope at 10 kV. The samples (solid) were set on carbon paste and sprayed with a 10 nm layer of Pt before observations.

Fourier-Transform Infrared (FTIR) spectra were obtained with a Vertex 70 apparatus made by Bruker. Spectra were acquired in transmission mode using polyethylene pressed discs (90 wt. % of polyethylene and 10 wt. % of geopolymer powders). The spectra were recorded between 50 to 800 cm^{-1} with a 4 cm^{-1} resolution and composed of 64 scans.

The XRD analysis was characterized using a Bruker-D8 Advance presenting a Bragg-Brentano geometry and Cu-K α 1 α 2 detector on powder samples. The analytical range was between 5 and 50° (2 θ) with a step of 0.02° (2 θ) and a dwell time of 1.5 s. The phase identification was performed with Powder Diffraction File (PDF) data from the International Center for Diffraction Data (ICDD).

High-resolution NMR experiments were performed on geopolymer powder at room temperature using a Bruker AVANCE-400 spectrometer, operating at 104.26 MHz for ^{27}Al signal and 79.49 MHz for ^{29}Si signal. A zirconia rotor ($\varnothing = 4$ mm) was used. The spinning

rate was 10 kHz. The ^{27}Al ($I = 5/2$) MAS NMR spectra were recorded after $p/8$ pulse irradiation ($1.5 \mu\text{s}$) using a 1- MHz filter to improve the signal/noise ratio. The ^{29}Si ($I = 1/2$) MAS NMR spectra were recorded after a $\pi/2$ -pulse irradiation ($4 \mu\text{s}$) using a 500 kHz filter to improve the signal/noise ratio. In each case, 400 scans were collected. The time between acquisitions was set to 5 and 10 s, respectively, to minimize saturation effects. A solution of AlCl_3 and Tetramethylsilane (TMS) were used as references for ^{27}Al and ^{29}Si . The deconvolution of NMR spectra was performed with the Winfit program (Bruker). The estimated errors for chemical shifts and relative areas are 1 ppm and 2 % respectively.

The mechanical strength was measured by compressive tests using an Instron 5969 with a 50 kN load cell at a constant speed of $0.5 \text{ mm}\cdot\text{min}^{-1}$, and was measured after seven days on six cylindrical samples for each parameter, with a 15 mm diameter and a 30 mm height [18].

The Young's modulus of the sample was determined by an ultrasonic contact echography technique detailed in previous work [19]. Samples with various thicknesses (15 to 20 mm) were placed between two couples of transducers (longitudinal and transverse) operating at 600 kHz.

III. RESULTS AND DISCUSSION

1. Influence of time and temperature on working properties

In order to elucidate the evolution and potential change of geopolymer over time and temperature, a geopolymer binder (M1) and three samples of geopolymer composites (M1W, M1G, M1WG) were demolded (7 days at $20 \text{ }^\circ\text{C}$) then stored at $20 \text{ }^\circ\text{C}$ ($\text{RH}=100 \%$) and $90 \text{ }^\circ\text{C}$ ($\text{RH} < 5\%$) and studied over time (0.5, 3, 9 and 20 months).

For instance, the visual aspect and the microstructure of the two samples (M1 and M1WG samples) are reported in **Table 1**. Both formulations present the same evolution of their color and microstructure over time and temperature. In fact, at $20 \text{ }^\circ\text{C}$ during 0.5 month, the sample M1 has a brown color and an homogenous microstructure typical of metakaolin based

geopolymer [20]. After aging (20 months at 20 °C), the color of the sample tending toward pale yellow is maybe due to some local reorganization of impurities in the M1 metakaolin [21, 22]. Storage at a higher temperature (at 90 °C during 0.5 or 20 months) induces the same behavior with pale yellow color and a less homogenous microstructure. This is due to the removal of physisorbed water leading to the formation of microstructural defects [23]. The same phenomenon is observed after aging.

The values of density and maximum stress measured over 20 months for the formulations M1, M1W, M1G, and M1WG are reported in **Figure 1** in order to evaluate the behavior of the several samples during these four conditions,. All the formulations present the same behavior in time and temperature. Indeed, a decrease of density (**Figure 1-a**) is observed over time and a more important decrease is measured at 90 °C. For instance, the M1WG sample presents a density of 1.663 g/cm³ after a 0.5 month storage at 20 °C that decreases to 1.350 g/cm³ after 20 months at 20 °C. It decreases even more at 90 °C during 20 months to reach 1.150 g/cm³. This suggests a transformation of structural entities forming the geopolymer network. The decrease of the density value with temperature and time can be also explained by a reinforcement of the structure consisting of a strengthening of network as in gel material [24]. Moreover, the compressive strength value of all samples (**Figure 1-b**) is similar over time at 20 °C. The decrease in compression values at 90 °C is due to the removal of physisorbed water. The water loss leads to the formation of larger pore sizes and a decrease in density. For instance, the M1WG sample presents a compressive strength equal to 29 and 26 MPa for a storage at 0.5 and 20 months at 20 °C. After a storage at a temperature of 90 °C, the compressive strength values decrease to 18 MPa at 0.5 month and to 12 MPa at 20 months. The specific stress is equal to 17 and 18 MPa.cm³g⁻¹, for a storage at 90 °C during 0.5 and 20 months, respectively which is similar to the specific stress at 20 °C (20 MPa.cm³g⁻¹) due to the decrease of compressive stress and density.

Consequently, the binder and the composites display the same changes over time and temperature. In order to understand this behavior, further structural and physico-chemical measurements will be undertaken on the binder M1.

2. Influence of time and temperature structure and the porosity and of the geopolymer binder

X-ray diffraction was performed. The XRD patterns are presented in **Figure 2**. For all samples, a broad reflection in the $2\theta \approx 28^\circ$ related to amorphous phase is observed. Furthermore, peaks related to crystalline phases, such as quartz, muscovite and anatase from metakaolin, are detected. No significant differences can be observed between the samples in function of time and temperature. For further structural informations, the studied samples were characterized by ^{27}Al and Si MAS-NMR spectroscopy. The obtained ^{27}Al MAS-NMR and ^{29}Si MAS-NMR spectra are presented in **Figure 3**. The chemical shift and percentages of the curve area of the various contributions are given in **Table 2**. Typical spectra of geopolymer materials are obtained showing that aluminum is predominantly four coordinated with two contributions at 48 and 57.5 ppm and in a minor part six coordinated with a contribution at 1 ppm. At 20 °C, the aging from 0.5 to 20 months leads to a quite similar spectrum. The contribution areas are also quite similar. At 90 °C during 0.5 months, the spectrum is broader than 20 °C with an increase of the tetrahedral Al component at 49 ppm from 9.1 to 13.5 %. This contribution is not due to quadrupolar effect and can be attributed to a distinct tetrahedral Al species as demonstrated by Vuono et al., [25] in the case of zeolite. This result suggests the potential nucleation of a minor zeolite type phase at 90 °C.

A 20 months curing at 90 °C, slight changes can be observed such as the increase of the tetrahedral Al component area at 48 ppm in the detriment of the component at 57 ppm from 13.5 to 18.2 % and a slight increase of the octahedral Al component at 1 ppm from 2.8 to 3.2 %. Generally, broad ^{29}Si MAS-NMR spectra are detected. The deconvolution evidences six

resonances: One at -79 ppm which can be attributed to unreacted or excess of silicate oligomers not bound to the gel and five components at -84,-89,-94,-100, -107 ppm assigned to $Q^4(n\text{Al})$ with n varying from 4 to 0, respectively, revealing a three-dimensional network (Q^4) characteristic of geopolymers materials [26]. The broad peak at -107 ppm is due to quartz from metakaolin [27]. As shown by ^{27}Al NMR-MAS data, at 20°C, no differences can be detected between 0.5 and 20 months. However, more changes can be observed at 90 °C with broader and more intense spectra revealing more disordered structure. Furthermore, it is noticed an increase of $Q^4(2\text{Al})$ and $Q^4(1\text{Al})$ to the detriment of $Q^4(3\text{Al})$ and $Q^4(4\text{Al})$ revealing a change in silicon and aluminum connectivity.

In order to understand the structural modifications occurring over time at 20 and 90 °C, the percentage ratio of $\text{Al}^{\text{IV}}/\text{Al}^{\text{VI}}$ from ^{27}Al MAS-NMR, and $Q^4(4\text{Al})/Q^4(2\text{Al})$ from ^{29}Si MAS-NMR were plotted as a function of storage conditions in **Figure 4**. At 20 °C, no change can be observed with increasing age either in $\text{Al}^{\text{IV}}/\text{Al}^{\text{VI}}$ (23 and 22 for 0.5 and 20 months, respectively) nor in $Q^4(2\text{Al})/Q^4(4\text{Al})$ percentage ratios (0.94 and 0.97 for 0.5 and 20 months, respectively), indicating a stable structure over time. However, at 90 °C for 0.5 months, an increase of $\text{Al}^{\text{IV}}/\text{Al}^{\text{VI}}$ ratio to 35 is noticed. This fact is due to the increase of the tetrahedral Al contribution at 49 ppm as shown above which is attributed to zeolite nucleation. Similarly, the $Q^4(2\text{Al})/Q^4(4\text{Al})$ percentage ratio increases to 1.33 revealing a change in Si and Al connectivity indicating a strengthening of ionic-covalent bonds. Indeed, Si-rich species ($Q^4(2\text{Al})$) are more stable and with higher strength than Al-rich species $Q^4(4\text{Al})$ [14,28].

A slight decrease of the two percentage ratios $\text{Al}^{\text{IV}}/\text{Al}^{\text{VI}}$ and $Q^4(2\text{Al})/Q^4(4\text{Al})$ is observed over time between the 0.5 and 20 months samples stored at 90 °C (29 and 1.09, respectively) indicating a structural reorganization and maturation over time not favoring the formation of zeolite.

In order to verify these hypotheses, FTIR spectroscopy in the range of 650-100 cm^{-1} was performed (**Figure 5**). The band near 110 cm^{-1} is due to stretching K-O bond [29]. The range 650–400 cm^{-1} is characteristic of rings made from $[\text{SiO}_4]$ and $[\text{AlO}_4]$ tetrahedra, and therefore zeolite structure [30], several broads and not well-resolved bands can be observed. A slight change can be observed in this region (especially at about 550 cm^{-1}) in the spectrum of the sample stored during 0.5 months at 90 °C. However, the absence of a definite peak in the region of zeolites reveals that the system does not contain a significant quantity of zeolite nanocrystals [31] which explains the very slight differences shown by XRD. pH value measurements were also undertaken. The sample stored 0.5 month at 20 °C has a pH value of 12.1 due to potassium ions that have not yet reacted [32]. This value decreases to 9.5 after 20 months of storage at 20 °C. This is significant in less unreacted species due to polycondensation reactions occurring over time. A 0.5 and 20 months storage leads respectively to a 9.8 and 9.4 pH value. The decrease of the pH values with the increase of temperature and time could be explained by either a lower amount of K^+ and OH^- not bonded to the matrix [15] or encapsulated in the solid skeleton of geopolymer due to a strengthening of the network.

The porosity and the pore size distribution of the samples after the four storage conditions are reported in **Figure 6**. Different pore size and total porosity are observed depending on time and temperature. The geopolymer M1 stored 0.5 months at 20 °C presents a total porosity equal to 40 % and a wide pore size distribution varying between 0.0078 and 0.2 μm . Two populations of pore size, 0.01-0.02 μm and 0.02-0.03 μm , can be distinguished which is typical of potassium solution and metakaolin-based geopolymer. A 20 months aging at the same temperature, leads to similar total porosity to 42 % and an increase of the 0.01-0.02 μm pore population. This fact is due to a densification of the network and maturation of the skeleton during the syneresis of the geopolymer gel [37]. After 0.5 months at 90 °C, most of

the pore sizes are between 0.02 to 0.03 μm . The elimination of the small pore size appears with an increase of the total porosity (54 %). This phenomenon occurs because of the evacuation of physisorbed and poral water in dry condition and high temperature that leads to a pore coalescence [33, 34]. After 20 months at 90 °C, the pore size increases significantly (mainly 0.1 μm) due to the pore coalescence in dry conditions. In a comparison with a storage of 0.5 month at 90 °C, a small decrease of total porosity is observed (45 %). This is probably due to the strengthening of the skeleton over time and temperature.

Consequently, aging at 90 °C seems to have a more significant effect on the local structure and pore size distribution than aging at 20 °C.

According to the previously discussed data, a mechanism of structural evolution scheme as a function of storage time and temperature can be established in **Figure 7**. Initially, at 20 °C, The network of the geopolymer binder is composed of a solid framework with different pore sizes due to the poral water containing K^+ ions, which can diffuse within this framework. Indeed, these K^+ ions ensure electronic neutrality by counterbalancing the aluminosilicate charges and are encapsulated in water molecules in interaction with physisorbed water. The studied geopolymer is characterized by high porosity and low pore size due to the use of a relatively low reactive alkaline solution and metakaolin. The sample presents a Young modulus (determined by the ultrasonic contact echography technique) equal to 3.5 GPa which is similar of the geopolymer Young modulus values obtained in literature with mechanical test [35] or ultrasonic contact echography technique [36]. The increase in rigidity is due to the densification with the syneresis of the material over time and temperature [37].

During aging over time (20 months), the elimination of the physisorbed water leads to a contraction of the solid network leading to a consolidation of the bonds and a decrease in pore size. This is in accordance with an improvement of the young modulus from 3.5 to 4 GPa. This contraction of the network and the higher number of pores induce a decrease of the

density. At 90 °C, the physisorbed water is removed very quickly, so there is a coalescence of the pore size. This induces a strengthening of the bonds ($E = 4.2$ GPa) and an increase in pore size manifested by a drastic decrease in density. This fact is accompanied by nucleation of metastable germs of zeolite as demonstrated by NMR and FTIR spectroscopies data. During aging at 90 °C, the phenomena are amplified and the Young's modulus increases (5.1 GPa) while the density decreases. This pore coalescence is responsible for the decrease in the mechanical strength value even if there is a reinforcement of the bonds. During the aging process, the mobility of K^+ ions is affected. At room temperature, the K^+ ions will be blocked in the pores, limiting their mobility and leading to a decrease of the pH value. Similarly, at 90 °C, the sudden removal of water results in a binding of these ions to the solid network causing the formation of $Si-O^- K^+$ bonds detected by FTIR spectroscopy.

IV. CONCLUSION

This study aims to elucidate the evolution of geopolymer binder (potassium metakaolin based geopolymer) and composites (binder and/or wollastonite and glass fibers) in the function of storage conditions (time and temperature) to evaluate their suitability for radioactive waste geological disposal applications. These applications require long term stability at 90 °C. All samples (binder and composites) display the same behavior at 20 and 90 °C for 0.5 and 20 months i.e a decrease of density and stability of mechanical strength over time and a slight decrease at 90 °C. In order to further explain this behavior, a focus was made on the mechanical, structural and pore size distribution evolution of the binder in the function of the studied storage conditions (time and temperature). It has been evidenced that:

- At 20 °C, after 0.5 months, the studied geopolymer is characterized by high porosity and low pore size and a Young modulus of 3.5 GPa.

- The aging of the sample during 20 months at the same temperature 20 °C does not induce structural changes as evidenced by NMR and FTIR spectroscopies indicating similar local-order with a strengthening of the skeleton. However, small changes can be detected. In fact, the porosity slightly increases with favored mesoporosity due to the elimination of the physisorbed water and the contraction of the solid network.

- The increase of storage temperature to 90°C during 0.5 months seems to induce the beginning of crystallization of metastable germs of zeolite. In parallel, the release of physisorbed water leads to an increase of the porosity rate and the pore size (coalescence of the pores), a decrease of the pH value, and a slight decrease of the specific compressive strength.

- The aging of the studied geopolymer during 20 months at 90 °C seems not promoting more crystallization of zeolite. An increase of pore size (until 0.1 μm) and Young's modulus (5.1 GPa) and a decrease of density are noticed.

Consequently, the aging of geopolymer at 20 °C or 90 °C seems not to degrade the structure and the properties of the final materials. The major changes concern the porosity and the pore size distribution. Further investigation (at a longer time or under hydrothermal conditions) of these materials will be undertaken.

Acknowledgment

We thank the French National Radioactive Waste Management Agency (Andra) for the funding of this research and Nicolas Texier-Doyen for helping us measure the Young Modulus with the ultrasonic contact echography technique

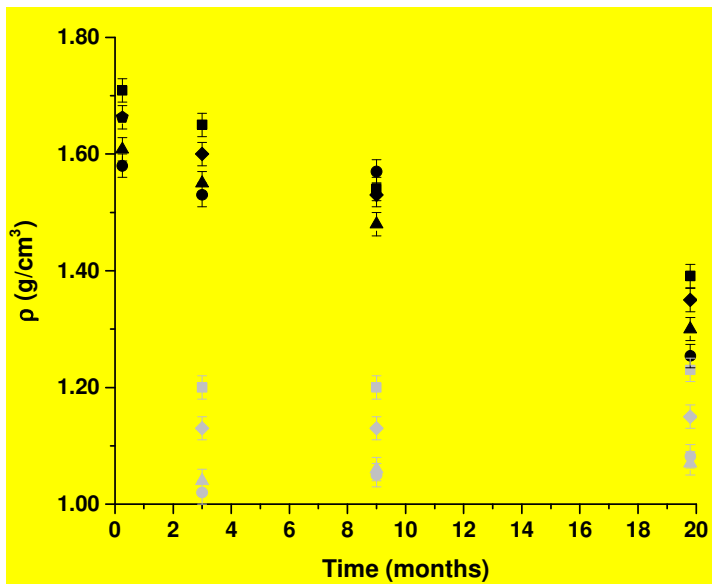
V. REFERENCES

[1] C. Dupuy, A. Gharzouni, I. Sobrados, N. Tessier-Doyen, N. Texier-Mandoki, X. Bourbon, S. Rossignol, 2020. Formulation of an alkali-activated grout based on Callovo-Oxfordian

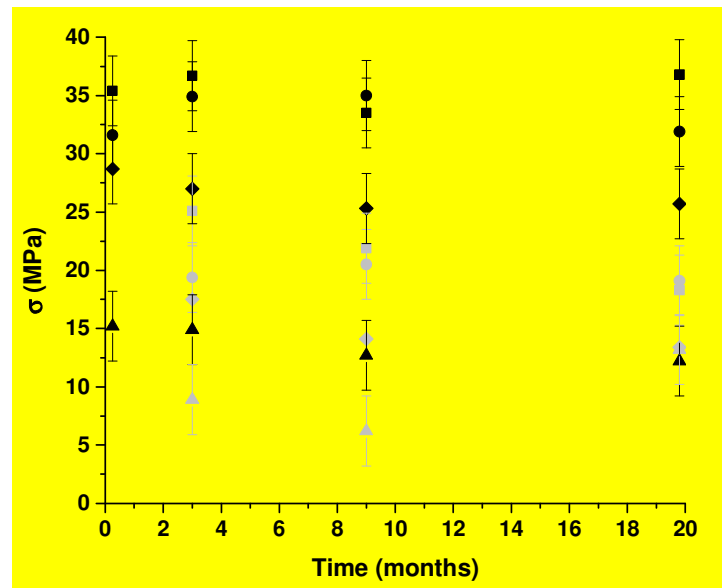
-
- argillite for an application in geological radioactive waste disposal. *Construction and Building Materials*. 232, 117170. 10.1016/j.conbuildmat.2019.117170.
- [2] J. Archez, N. Texier-Mandoki, X. Bourbon, J.F. Caron, S. Rossignol, 2020. Adaptation of the geopolymer composite formulation binder to the shaping process. *Materials Today Communications*. 25, 101501. 10.1016/j.mtcomm.2020.101501.
- [3] T. M. Tognonvi, S. Petlitckaia, A. Gharzouni, M. Fricheteau, N. Texier-Mandoki, X. Bourbon, S. Rossignol, High-temperature resistant, argillite-based, alkali-activated materials with improved post-thermal treatment mechanical strength, *Clays and Clay Minerals*. 68 (2020) 211-219. doi:10.1007/s42860-020-00067-9.
- [4] C. Dupuy, A. Gharzouni, S. Rossignol, Thermal resistance of argillite-based alkali-activated materials. Part 1: Effect of calcination processes and alkali cation, *Materials Chemistry and Physics*. 217 (2018) 323-333. 10.1016/j.matchemphys.2018.06.079.
- [5] M. Behzad, "Geopolymer Technology, from Fundamentals to Advanced Applications: A Review." *Materials Technology: Advanced Performance Materials*. 24 (2009) 79-87. 10.1179/175355509X449355.
- [6] Y.M Liew, H. Kamarudin, A.M. Mustafa Al Bakri, M. Luqman, I. Khairul Nizar, C.Y. Heah, Investigating the possibility of utilization of kaolin and the potential of metakaolin to produce green cement for construction purposes, *Aust J Basic Appl Sci*. 5 (2011) 441-449.
- [7] R. Wan-Wendner, Aging concrete structures: a review of mechanics and concepts, *Bodenkultur*. 69 (2018) 175-199. 10.2478/boku-2018-0015.
- [8] M. Niveditha, S. Koniki, 2020. Effect of durability properties on geopolymer concrete- a review. *ICMED 2020*. 184, 01092. <https://doi.org/10.1051/e3sconf/202018401092>.
- [9] R. Cioffi, L. Maffucci, L. Santoro, Optimization of geopolymer synthesis by calcination and polycondensation of a kaolinitic residue *Resources, Conservation and Recycling*. 40 (2003) 27–38. 10.1016/S0921-3449(03)00023-5.
- [10] P. Steins, A Poulesquen, F. Frizon, O. Diat, J. Jestin, J. Causse, D. Lambertin, S. Rossignol, Effect of Aging and Alkali Activator on the Porous Structure of a Geopolymer, *J. Appl. Crystallogr*. 47 (2014) 316-324. 10.1107/S160057671303197X.
- [11] Z.F. Farhana, H. Kamarudin, A. Rahmat, A.M. Al Bakri, The relationship between water absorption and porosity for geopolymer paste, *Materials Science Forum*. 803 (2015) 166-172. 10.4028/www.scientific.net/MSF.803.166
- [12] S. Thokchom, P. Ghosh, S. Ghosh, Effect of water absorption, porosity and sorptivity on durability of geopolymer mortars, *ARPN Journal of engineering and Applied Sciences*. 4 (2009) 28-32.
- [13] J. Melar, G. Renaudin, F. Leroux, A. Hardy-Dessources, J.M. Nedelec, C. Taviot-Gueho, E. Petit, P. Steins, A. Poulesquen, F. Frizon, The Porous Network and its Interface inside Geopolymers as a Function of Alkali Cation and Aging, *J. Phys. Chem. C*. 119 (2015) 17619-17632. 10.1021/acs.jpcc.5b02340.
- [14] G. Kovalchuk, A. Fernandez-Jiménez, A. Palomo, Alkali-activated fly ash : effect of thermal curing conditions on mechanical and microstructural development – Part II., *Fuel*. 86 (2007) 315-222. 10.1016/j.fuel.2006.07.010.
- [15] I. Lancellotti, M. Catauro, C. Ponzoni, F. Bollino, C. Leonelli, Inorganic polymers from alkali activation of metakaolin : effect of setting and curing on structure, *Journal of Solid State Chemistry*. 200 (2013) 341-348. 10.1016/j.jssc.2013.02.003.
- [16] J. Archez, N. Texier-Mandoki, X. Bourbon, J.F Caron., S. Rossignol, 2020. Influence of the aluminum concentration, wollastonite and glass fibers on geopolymer composites workability and mechanical properties. *Construction and Building Materials*. 257, 119511. 10.1016/j.conbuildmat.2020.119511.

-
- [17] C. Dupuy, J. Havette, A. Gharzouni, N. Texier-Mandoki, X. Bourbon, S. Rossignol, Metakaolin-based geopolymer: formation of new phases influencing the setting time with the use of additives, *Construction and Building Materials*. 200 (2019) 272-281. 10.1016/j.conbuildmat.2018.12.114.
- [18] ASTM D1633 - 17 "Standard Test Methods for Compressive Strength of Molded Soil-Cement Cylinders"
- [19] C. Dupuy, A. Gharzouni, I. Sobrados, N. Tessier-Doyen, N. Texier-Mandoki, X. Bourbon, S. Rossignol, 2020. Formulation of an alkali-activated grout based on Callovo-Oxfordian argillite for an application in geological radioactive waste disposal. *Construction and Building Materials*. 232, 117170. 10.1016/j.conbuildmat.2019.117170.
- [20] A. Gharzouni, B. Samet, S. Baklouti, E. Joussein, S. Rossignol, Addition of low reactive clay into metakaolin-based geopolymer formulation: Synthesis, existence domains and properties, *Powder technology*. 288 (2016) 212-220. 10.1016/j.powtec.2015.11.012.
- [21] P. Weber, Fading concrete block surfaces - Why do black, colored and gray concrete block surfaces appear lighter in the course of time? *Concrete Plant and Precast Technology*. 80 (2014) 34-35.
- [22] D. Kong, J. Sanjayan, K. Sagoe-Crentsil, Comparative performance of geopolymers made with metakaolin and fly ash after exposure to elevated temperatures, *Cem.Concr. Res.* 37, (2007) 1583-1589. 10.1016/j.cemconres.2007.08.021.
- [23] C. Kuenzel, L.J. Vandeperre, S. Donatello, A. R. Boccaccini, C. Cheeseman, Ambient temperature drying shrinkage and cracking in metakaolin-based geopolymers, *J. Am. Ceram. Soc.* 95 (2012) 3270-3277. 10.1111/j.1551-2916.2012.05380.x.
- [24] M. Tohoué Tognonvi, *Physico-chimie de la gélification du silicate de sodium en milieu basique*, 2009, Université de Limoges.
- [25] D. Vuono, L. Pasqua, F. Testa, R. Aiello, A. Fonseca, T.I. Korányi, J.B. Nagy, Influence of NaOH and KOH on the synthesis of MCM-22 and MCM-49 zeolites, *Microporous and Mesoporous Materials*. 97 (2006) 78-87. 10.1016/j.micromeso.2006.07.015.
- [26] P. Duxson, J.L. Provis, G.C. Lukey, F. Separovic, J.S.J. van Deventer, ²⁹Si NMR Study of Structural Ordering in Aluminosilicate Geopolymer Gels, *Langmuir*. 21 (2005) 3028-3036. 10.1021/la047336x.
- [27] I. Lecomte, M. Liégeois, A. Rulmont, R. Cloots, F. Maseri, Synthesis and characterization of new inorganic polymeric composites based on kaolin or white clay and on ground-granulated blast furnace slag, *Journal of Materials Research*. 18 (2003) 2571-2579. 10.1557/jmr.2003.0360.
- [28] Á. Palomo, S. Alonso, A. Fernandez-Jiménez, I. Sobrados, J. Sanz, Alkaline Activation of Fly Ashes: NMR Study of the Reaction Products, *J. Am. Ceram. Soc.* 87 (2004) 1141-1145. 10.1111/j.1551-2916.2004.01141.x
- [29] M. Zhang, S.A.T. Redfern, E.K.H. Salje, M.A. Carpenter, C. L. Hayward, Thermal behavior of vibrational phonons and hydroxyls of muscovite in dehydroxylation: In situ high-temperature infrared spectroscopic investigations, *American Mineralogist*. 95 (2010) 1444-1457. 10.2138/am.2010.3472
- [30] M. Krol, J. Minkiewicz, W. Mozgawa, IR spectroscopy studies of zeolites in geopolymeric materials derived from kaolinite, *Journal of Molecular Structure*. 1126 (2016) 200-206. 10.1016/j.molstruc.2016.02.027.
- [31] C.A. Rees, J.L. Provis, G.C. Lukey, S.J.J. van Deventer, Attenuated Total Reflectance Fourier Transform Infrared Analysis of Fly Ash Geopolymer Gel Aging, *Langmuir*. 23 (2007) 8170-8179. doi.org/10.1021/la700713g.

-
- [32] A. Gharzouni, E. Joussein, B. Samet, S. Baklouti, S. Rossignol, Effect of the reactivity of alkaline solution and metakaolin on geopolymer formation, *Journal of Non-Crystalline Solids*. 410 (2014) 127-134. 10.1016/j.jnoncrysol.2014.12.021.
- [33] J. Ye, W. Zhang, D. Shi, Effect of elevated temperature on the properties of geopolymer synthesized from calcined ore-dressing tailing of bauxite and ground-granulated blast furnace slag, *Construction and Building Materials*. 69 (2014) 41-48. 10.1016/j.conbuildmat.2014.07.002
- [34] D.S. Perera, O. Uchida, E.R. Vance, K.S. Finnie, Influencing of curing schedule on the integrity of geopolymers, *Journal of Materials Science*. 42, (2007) 3099-3106. 10.1007/s10853-006-0533-6.
- [35] P. Duxson, J.L. Provis, G. C. Lukey, S.W. Mallicoat, W.M. Kriven, J.S.J. Deventer, Understanding the relationship between geopolymer composition, microstructure and mechanical properties, *Coll. Surf. A: Physicochem. Eng. Aspect*. 269 (2005), 7-58. 10.1016/j.colsurfa.2005.06.060.
- [36] P. Duxson, J.L. Provis, G. C. Lukey, S.W. Mallicoat, W.M. Kriven, J.S.J. Deventer, Understanding the relationship between geopolymer composition, microstructure and mechanical properties, *Coll. Surf. A: Physicochem. Eng. Aspect*. 269 (2005), 7-58. 10.1016/j.colsurfa.2005.06.060.
- [37] C. Jeffrey Brinker, G.W. Scherer, *Sol-gel science, the physics and chemistry of sol-gel processing*, Elsevier Science Publishing, 1990. 10.1016/C2009-0-22386-5.



(a)



(b)

Figure 1. Values of the (a) density ($\pm 0.02 \text{ g/cm}^3$) and (b) compressive strength ($\pm 3 \text{ MPa}$) as a function of time for the compositions (●) M1, (■) M1W, (▲) M1G, (◆) M1WG stored at (●, ■, ▲, ◆) 20 °C and (●, ■, ▲, ◆) 90 °C.

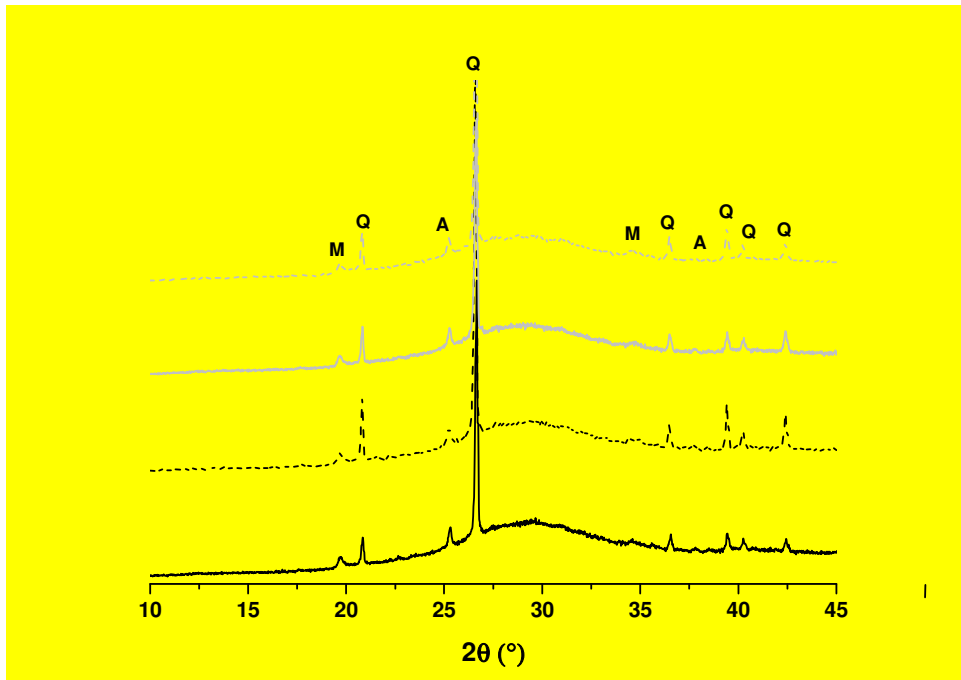
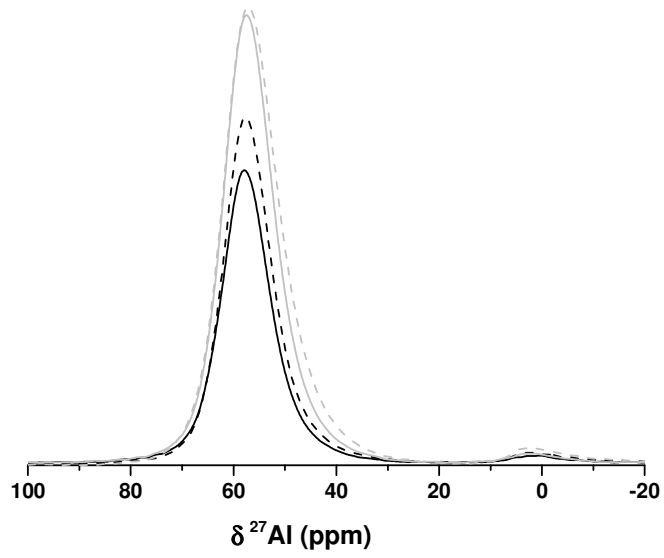
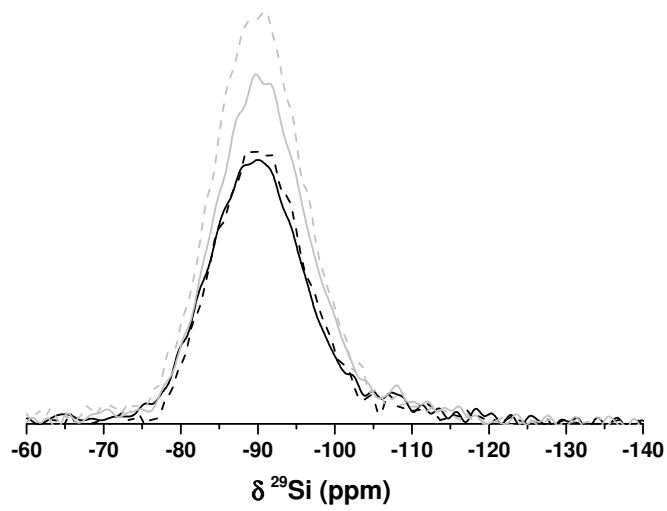


Figure 2. X-ray patterns of the geopolymer M1 stored at — 20°C, 0.5 months, ---20 °C, 20 months, — 90°C, 0.5 months and - - - 90°C, 20 months (PDF files: Quartz (01 – 083 – 2465), M: Muscovite (00 – 003 – 0849), A: Anatase (01 – 071 – 1166),



(a)



(b)

Figure 3. (a) ^{27}Al and (b) ^{29}Si NMR spectra of the geopolymer M1 stored at — 20°C , 0.5 months, --- 20°C , 20 months, — 90°C , 0.5 months and - - - 90°C , 20 months.

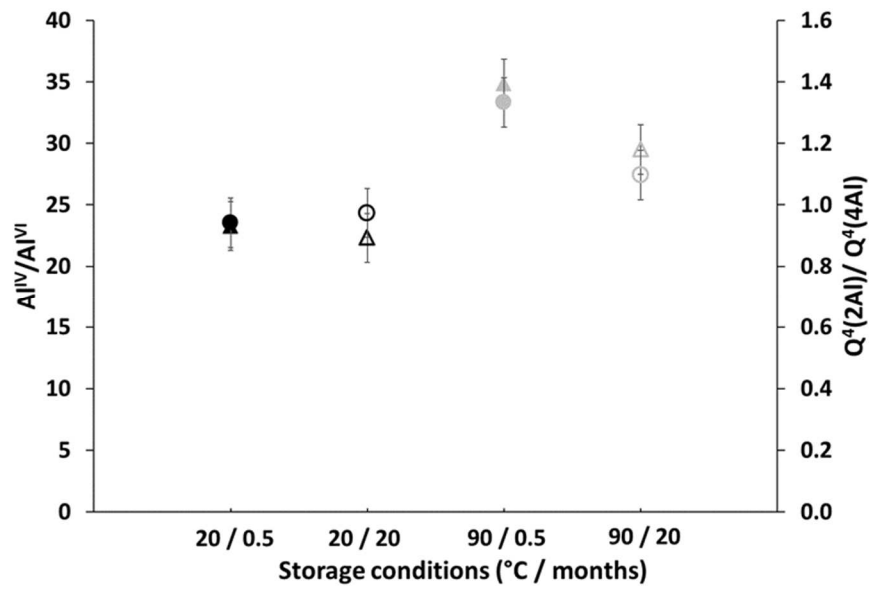


Figure 4. values of ● $Q^4(2Al)/Q^4(4Al)$ (^{29}Si NMR), ▲ Al^{IV}/Al^{VI} (^{27}Al NMR) of the geopolymer M1 stored at ● 20°C, 0.5 months, ○ 20 °C, 20 months, ● 90°C, 0.5 months and ○ 90°C, 20 months.

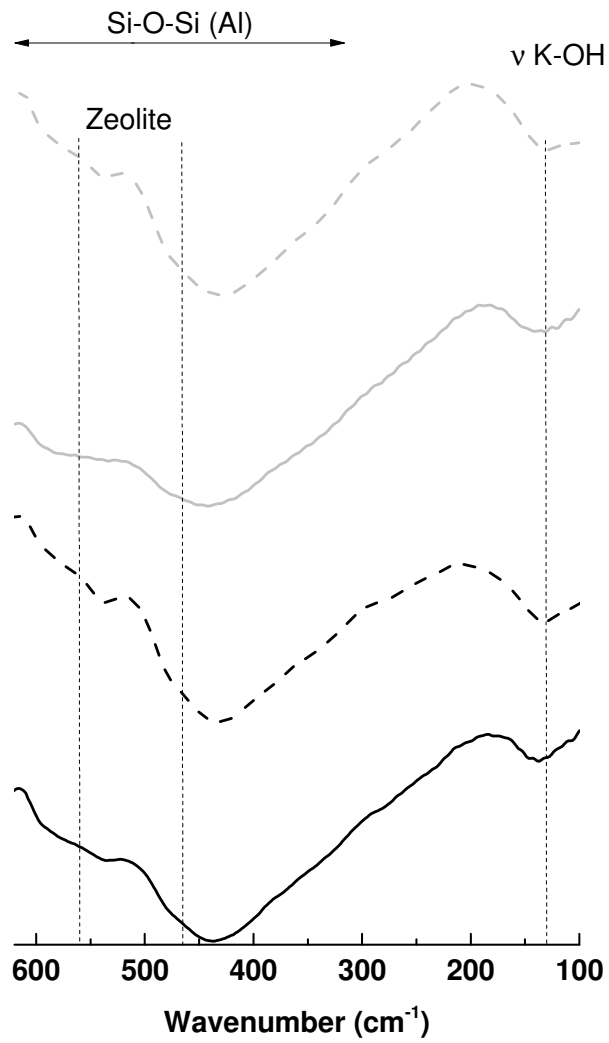


Figure 5. Low frequency FTIR spectra of the geopolymer M1 stored at — 20°C, 0.5 months, --- 20 °C, 20 months, — 90°C, 0.5 months and . . . 90°C, 20 months.

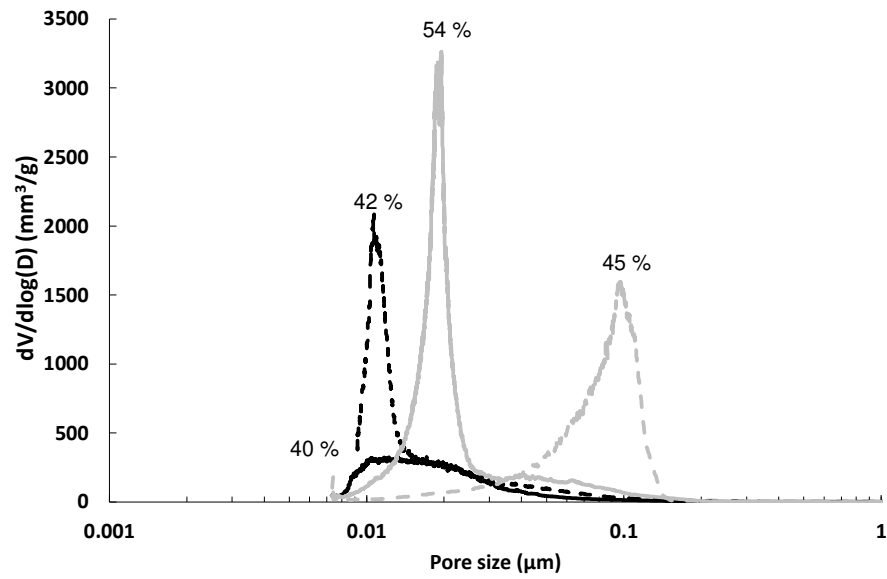


Figure 6. Values of the pore volume ($dV/d\log(D)$) as a function of the pore size of the geopolymer M1 stored at — 20°C, 0.5 months, --- 20 °C, 20 months, — 90°C, 0.5 months and === 90°C, 20 months and values of total porosity (%).

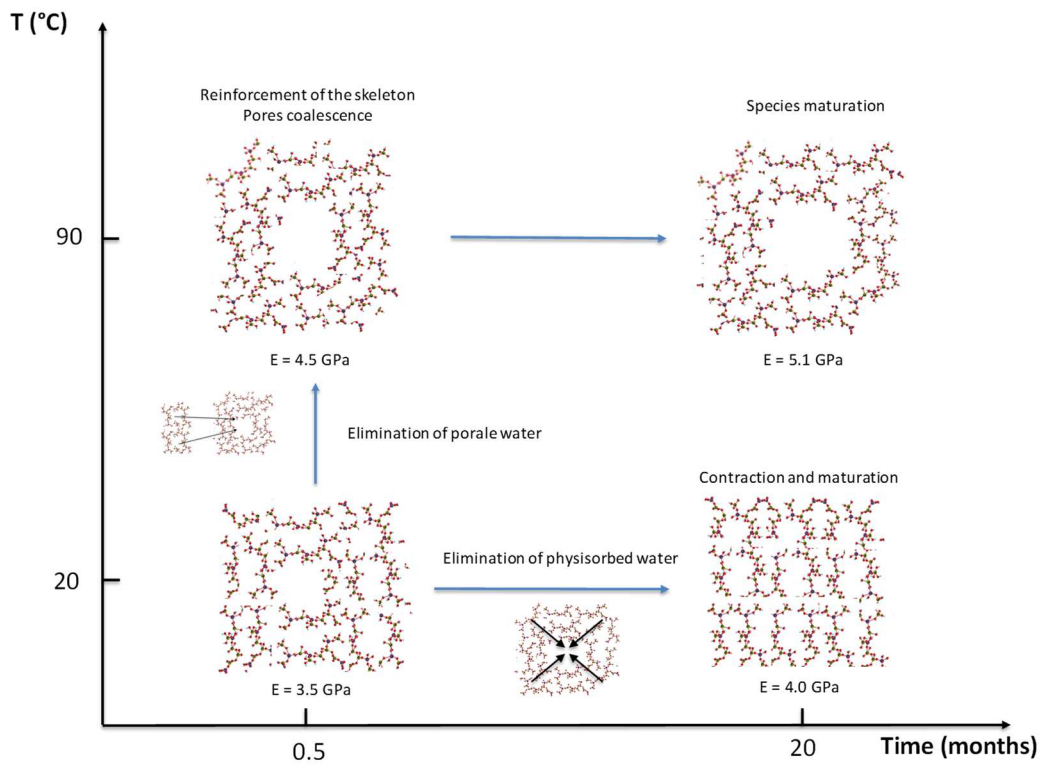


Figure 7. Schematic image of the aging mechanisms of a geopolymer at 20 and 90 °C.

Table 1. Photos of samples ($Si/Al = 1.62$) and value of density measured in different storage conditions





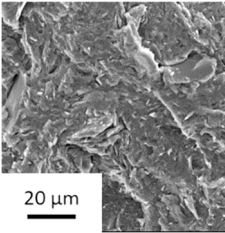
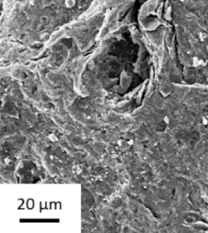
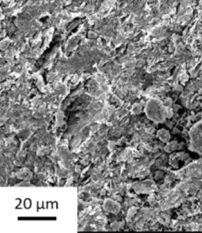
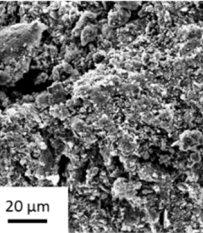




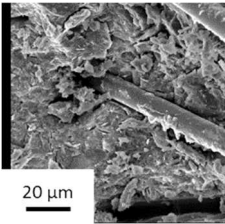
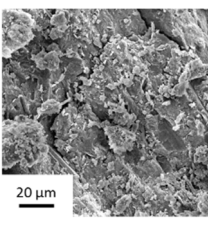
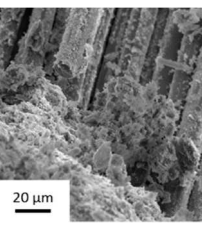
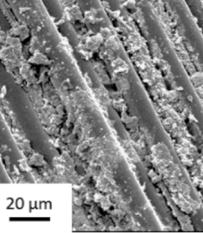
		Storage condition (°C/ months)	20 / 0.5	20 / 20	90 / 0.5	90 / 20
M1	Photo ($\phi = 15$ mm)					
	SEM photo	 20 μ m	 20 μ m	 20 μ m	 20 μ m	
M1WG	Photo ($\phi = 15$ mm)					
	SEM photo	 20 μ m	 20 μ m	 20 μ m	 20 μ m	

Table 2. ^{27}Al and ^{29}Si NMR chemical shift and percentage of the curve area determined with a deconvolution of spectra for the M1 samples in different conditions of storage

Storage conditions (°C/ months)	Chemical shift (ppm) ^{27}Al	Area (%) ^{27}Al	Chemical shift (ppm) ^{29}Si	Area (%) ^{29}Si
20 / 0.5	57.8	87.4	-78.1	3.4
	48.0	8.5	-84.0	23.8
	1.0	4.1	-89.5	37.8
			-94.5	22.4
			-100.0	8.6
			-107.0	3.9
20 / 20	57.6	86.6	-79.7	2.7
	48.0	9.1	-84.5	24.6
	1.0	4.3	-89.8	37.2
			-94.5	23.9
			-100.0	8.6
			-107.8	3.0
90 / 0.5	57.5	83.7	-79.0	3.1
	49.0	13.5	-84.2	19.3
	1.0	2.8	-89.5	38.5
			-94.5	25.8
			-100	9.9
			-107.5	3.5
90 / 20	57.2	78.5	-78.1	4.3
	48.0	18.2	-84.5	22.6
	1.0	3.3	-89.6	37.6
			-94.5	24.7
			-100.0	8.4
			-107.0	2.4